

# MOTOR PATTERNS OF LABRIFORM LOCOMOTION: KINEMATIC AND ELECTROMYOGRAPHIC ANALYSIS OF PECTORAL FIN SWIMMING IN THE LABRID FISH *GOMPHOSUS VARIUS*

MARK W. WESTNEAT\* AND JEFFREY A. WALKER

Department of Zoology, Field Museum of Natural History, Roosevelt Road at Lake Shore Drive, Chicago, IL 60605-2496, USA

Accepted 21 April 1997

## Summary

Labriform locomotion is a widespread swimming mechanism in fishes during which propulsive forces are generated by oscillating the pectoral fins. We examined the activity of the six major muscles that power the pectoral fin of the bird wrasse *Gomphosus varius* (Labridae: Perciformes). The muscles studied included the fin abductors (arrector ventralis, abductor superficialis and abductor profundus) and the fin adductors (arrector dorsalis, adductor superficialis and adductor profundus). Our goals were to determine the pattern of muscle activity that drives the fins in abduction and adduction cycles during pectoral fin locomotion, to examine changes in the timing and amplitude of electromyographic (EMG) patterns with increases in swimming speed and to correlate EMG patterns with the kinematics of pectoral fin propulsion. EMG data were recorded from three individuals over a range of swimming speeds from 15 to 70 cm s<sup>-1</sup> (1–4.8 TL s<sup>-1</sup>, where TL is total body length). The basic motor pattern of pectoral propulsion is alternating activity of the antagonist abductor and adductor groups. The downstroke is characterized by activity of the arrector ventralis muscle before the other abductors, whereas the upstroke involves nearly

synchronous activity of the three adductors. Most EMG variables (duration, onset time, amplitude and integrated area) showed significant correlations with swimming speeds. However, the timing and duration of muscle activity are relatively constant across speeds when expressed as a fraction of the stride period, which decreases with increased velocity. Synchronous recordings of kinematic data (maximal abduction and adduction) with EMG data revealed that activity in the abductors began after maximal adduction and that activity in the adductors began nearly synchronously with maximal abduction. Thus, the pectoral fin mechanism of *G. varius* is activated by positive work from both abductor and adductor muscle groups over most of the range of swimming speeds. The adductors produce some negative work only at the highest swimming velocities. We combine information from pectoral fin morphology, swimming kinematics and motor patterns to interpret the musculoskeletal mechanism of pectoral propulsion in labrid fishes.

Key words: swimming, locomotion, kinematics, electromyography, bird wrasse, *Gomphosus varius*, Labridae, biomechanics, pectoral fin.

## Introduction

Many fishes use their pectoral fins as the primary propulsors for aquatic locomotion. The mechanism of force generation by the pectoral fins reflects a hierarchy of design levels (Westneat, 1996). Hydrodynamic forces generated by the pectoral fins are determined by the complex kinematics of the fins, by fin shape and orientation, and by swimming speed. Fin kinematic patterns are determined by the interaction between the architecture of the pectoral girdle (Geerlink, 1989; Westneat, 1996), the mechanical properties of the fin tissues and the motor patterns of the muscles driving the fins. Pectoral fin kinematic patterns are the most thoroughly investigated of these design levels. Labriform propulsion has traditionally been categorized into two general forms on the basis of the

pattern of fin kinematics and associated steady force mechanism: drag-based rowing and lift-based flapping (Blake, 1983). In addition to the steady forces, several authors have suggested that unsteady forces contribute to the force balance of the pectoral fin. Possible unsteady forces include the acceleration reaction (Daniel, 1984; Gibb *et al.* 1994), the jet reaction (Geerlink, 1983; Daniel and Meyhofer, 1989) and delayed stall (Walker and Westneat, 1997).

Kinematic studies indicate that pectoral fin movements are variable among species and within species across a range of speeds (Webb, 1973; Geerlink, 1989; Gibb *et al.* 1994; Drucker and Jensen, 1996; Walker and Westneat, 1997). For example, Webb (1973) identified two different pectoral

\*e-mail: westneat@fmnh.org.

movement patterns in the surfperch *Cymatogaster aggregata*, both of which were used for forward propulsion. Geerlink (1989) compared the pectoral morphology and kinematics of three labroid fishes and found a high level of variability in fin motions. Although he did not have electromyographic data, he suggested that 'cybernetic factors' or neuromuscular control of behavior explained the kinematic differences among species. In a third study, it was shown that the frequency, stroke angle, angle of attack and other features of the pectoral stroke of the labrid *Gomphosus varius* are variable within an individual across speeds (Walker and Westneat, 1997).

These studies reveal behavioral variation that is central to the mechanics of generating thrust with the pectoral fins. Clearly, research on the morphological and neural basis of this variation is the critical next step to an understanding of labriform propulsion in fishes. Important features of pectoral anatomy have been described (Geerlink, 1989; Westneat, 1996), but few data on the motor patterns of pectoral muscles during labriform propulsion have been published. The basic electromyographic (EMG) pattern of the abductors and adductors was described by Westneat (1996), and Drucker and Jensen (1997) compared the pectoral EMGs of two surfperch species, each swimming at a single speed. More detailed study of pectoral motor patterns may yield important insights into locomotor function. Recent EMG studies of the myomeres in fishes (Jayne and Lauder, 1995; Rome *et al.* 1993; Wardle *et al.* 1995) were used to correlate muscle activity along the body with important kinematic variables such as local vertebral bending. These data also played a central role in the calculation of the work done by muscle during swimming (Altringham *et al.* 1993; Rome and Swank, 1992). Similarly, research on muscle mechanics during flight in birds (Dial *et al.* 1991; Tobalske, 1995) and insects (Mizisin and Josephson, 1987; Tu and Dickinson, 1994) has used EMG data and *in vitro* recordings of muscle activity to interpret the mechanics of flight and to evaluate the work done by flight muscle. Attempts to understand the mechanics of labriform locomotion in fishes require data on the motor patterns of the muscles that drive the flapping fins.

In the present paper, we describe the EMG patterns of the pectoral muscles in the labrid fish *Gomphosus varius* across a range of swimming speeds. We ask several fundamental questions regarding the motor patterns of pectoral propulsion in fishes. What is the sequence of muscle activity that drives the fins in abduction and adduction cycles during pectoral flapping? How do the motor patterns change with changes in swimming velocity? And how are the patterns of muscle activity associated with particular motions of the fin during the pectoral fin stroke? To answer these questions, electromyograms of the six major pectoral muscles were recorded and synchronized with video analysis. We use the association of EMG data with three-dimensional kinematic data (Walker and Westneat, 1997) to interpret the basic musculoskeletal mechanism of pectoral fin propulsion in labrid fishes.

## Materials and methods

### Electromyography

Three bird wrasses (*Gomphosus varius* Lacepède), ranging in size from 12.4 to 16.5 cm total length (*TL*), were purchased from aquarium suppliers. Fishes were maintained in 200 l aquaria, at a temperature of 25–28 °C, on a diet of dried shrimp and pellets. Fishes were anesthetized using methane sulfonate (FinQuel, Aldrich). The experiments involved synchronized recording of electromyograms and video recording of locomotor behavior (Fig. 1). For recording electromyograms, bipolar, fine wire electrodes were constructed from 0.05 mm diameter, insulated, stainless-steel wire. Insulation was stripped from a 0.5 mm section of each wire to form an electrode tip with two bare wire sections 1.0 mm apart. Electrodes were threaded through a 25 gauge needle for implantation into muscles. Care was taken to standardize electrode construction in order to minimize signal variation due to electrodes.

We measured EMGs in three lateral muscles, the arrector ventralis, the abductor superficialis and the abductor profundus (Fig. 2A,B), and three medial muscles, the arrector dorsalis, the ventral portion of the adductor superficialis and the adductor profundus (Fig. 2C,D). Electrodes were implanted into the muscles of the left pectoral fin (Fig. 2) by sliding the syringe needle beneath the scales, through the skin and into the target muscle. Electrodes were implanted so as to orient the sensory tips of the electrodes parallel to the muscle fiber direction. Electrode wires were run dorsally to a suture at the base of the first dorsal spine, where they were glued together to form a single cable that extended 40–50 cm from the fish. *Post-mortem* dissection confirmed the placement of electrode wires in the target muscles.

After recovery (for a minimum of 2 h), the fish swam in a flow tank (Vogel and LaBarbera, 1978) with a volume of 360 l and working area dimensions of 30 cm×30 cm×120 cm (Fig. 1). Swimming speeds were 15–70 cm s<sup>-1</sup>, equivalent to a size-specific speed range of 1–4.8 total body lengths s<sup>-1</sup> (*TL*s<sup>-1</sup>), at Reynolds numbers of approximately 11×10<sup>3</sup> to 69×10<sup>3</sup> calculated using total body length. These speeds were always below the critical swimming speed for *G. varius*, which is approximately 6 *TL*s<sup>-1</sup> (M. W. Westneat and J. A. Walker, unpublished data). Fishes used only pectoral fin propulsion at all speeds measured and never used body–caudal fin propulsion. The stroke plane angles and frequencies of the fin beats during the EMG experiments were similar to those for free-swimming fishes (Walker and Westneat, 1997), although the frequency increased slightly more rapidly as speed increased.

EMG signals were amplified by a factor of 5000–10 000 using AM Systems model 1700 amplifiers, and recorded on a TEAC eight-channel model RD-130TE DAT tape recorder (Fig. 1). EMGs were later digitized by an NB-MIO-16 analog-to-digital converter driven by LabVIEW virtual instrument software (National Instruments Corp., Austin, Texas). The sample rate was 5000 points s<sup>-1</sup> channel<sup>-1</sup>. The digital record

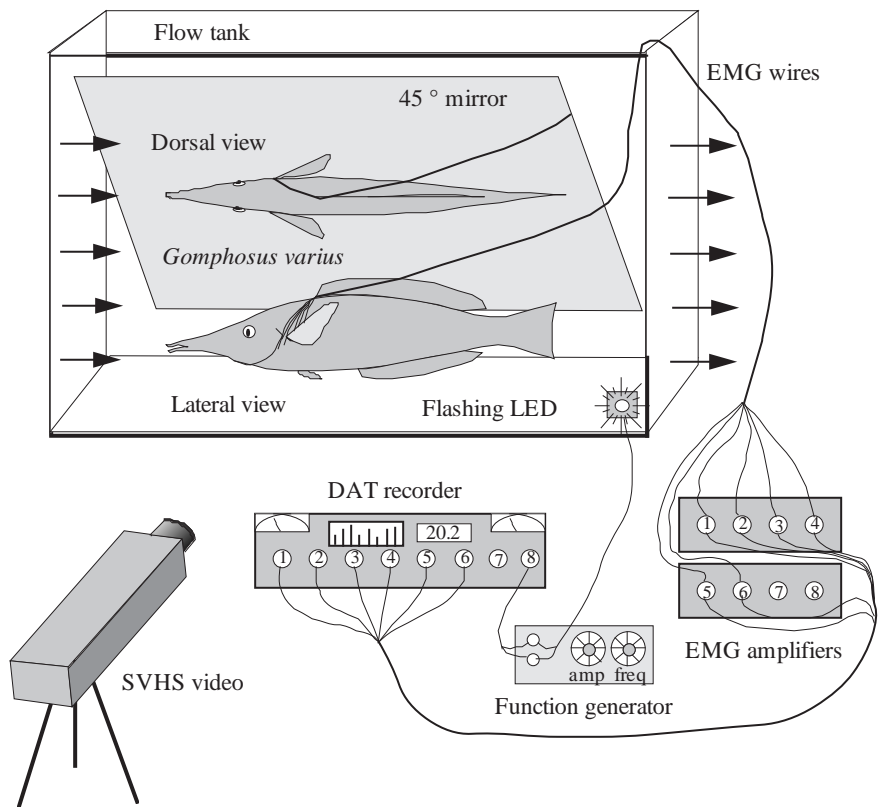


Fig. 1. Experimental protocol for synchronized kinematics and electromyography of labriform locomotion in *Gomphosus varius*. The 8 Hz square-wave pulse of the function generator splits to the electromyographic (EMG) tape recorder and to the flashing light-emitting diode (LED), allowing synchronization of video images and EMG records.

was then analyzed using a six-channel analysis algorithm custom-designed (M. Westneat) using the LabVIEW virtual instrument library. Analysis involved filtering the data with a high-pass Butterworth filter set at a sample rate of 5000 Hz and a low cut-off frequency of 60 Hz. Each channel was visually inspected to determine the baseline noise level, and a cut-off amplitude was chosen, below which all values were set to zero. This allowed repeatable identification of the onset and offset of each muscle burst within an EMG record.

Five locomotor cycles (complete fin beats) were analyzed for each fish at each of 6–8 flow tank speeds, for a total of 105 fin beats analyzed. The muscular motor pattern of each fin beat consisted of the measurement of 29 EMG variables in five groups (Fig. 3): (1) the duration (ms) of muscle activity; (2) the onset time (ms) of other muscles relative to arrector ventralis activity, the initiator of a fin-beat cycle; (3) the mean signal amplitude (mV) of each burst of activity; (4) the area under the rectified (absolute value) EMG trace (in mV ms; computed by multiplying the mean signal amplitude of the rectified spikes by the duration of the burst); and (5) the onset times of the abductor muscles relative to maximal fin adduction and the onset times of the adductor muscles relative to maximal fin abduction. Although electrode construction and implantation were standardized as much as possible, comparison of signal amplitudes or rectified areas among muscles and among individuals is confounded by potential variation in electrode structure and EMG implant position. However, we analyzed the amplitude variables for the overall patterns associated with swimming speed.

#### Synchronized kinematics and EMG

Video recordings were made simultaneously with EMG recordings to document fin motions in dorsal and lateral view (Fig. 1). To synchronize video-tape with EMG signals, a 5 V square wave from a function generator pulsing at 8 Hz was fed simultaneously to a channel of the EMG tape deck and to a flashing light-emitting diode (LED) on the video view. Dorsal views were obtained by placing a mirror at 45° to the base of the flow tank (Fig. 1). Videos were recorded using a Panasonic AG-450 SVHS camera at a shutter speed of 1/1000 s and a frame rate of 60 video fields  $s^{-1}$ . Swimming kinematic patterns were digitized using a Panasonic AG-1970 tape deck at 60 images  $s^{-1}$ . A TelevEyes/Pro video scan converter with genlock (Digital Vision Corp.) overlaid video and Macintosh computer images on a Sony PVM-1340 monitor. Custom-designed video-digitizing software for the Macintosh (J. A. Walker) was used to select coordinates from the video image. Digitized points were recorded for the fin tip and fin base in order to calculate the points at which the amplitude (angular rotation) of the fin was at maximum abduction and maximum adduction. These data were used for determining the timing of EMG signals relative to fin stroke kinematic maxima. To examine the association of EMG timing with kinematic events across speeds, we computed the cycle onset and duty factor of each muscle. These parameters were calculated as the muscle onset times and durations divided by the total stride duration (time from maximum adduction to the next maximum adduction).

The accuracy of synchronized EMG and video recordings

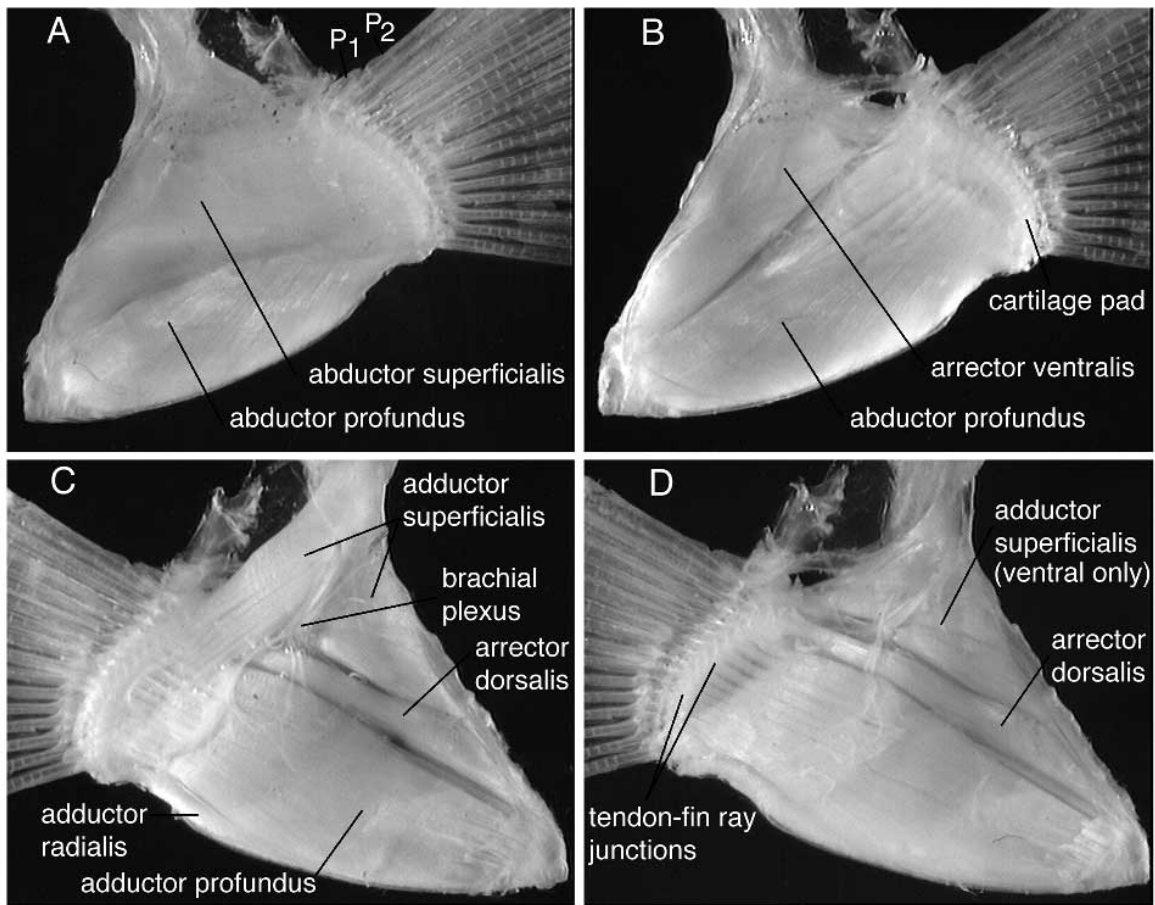


Fig. 2. Morphology of the pectoral muscles of *Gomphosus varius*. (A) Lateral superficial view of the left pectoral fin, showing the abductor superficialis and abductor profundus. P<sub>1</sub>, P<sub>2</sub>, first and second pectoral rays. (B) Deep lateral view, with the abductor superficialis removed to reveal the arrector ventralis. (C) Medial superficial view of the left pectoral fin, showing the adductor superficialis (both dorsal and ventral parts), arrector dorsalis, adductor profundus and adductor radialis. Note the motor nerves of the brachial plexus that innervate the muscles of interest. (D) Deep medial view, with the dorsal portion of the adductor superficialis removed to reveal the tendons of the arrector ventralis and adductor profundus. Each image is 5 cm wide.

was maximally limited by the interfield time of the video, at 16.67 ms. However, because the LED flashed at 8 Hz and the video frame rate was 60 Hz, the light was not synchronized with the frame rate, enabling a more accurate estimation of the timing of the light pulse, usually to within half an interfield time, or 8 ms.

We searched for significant associations between swimming velocity and each of the 29 EMG variables by performing least-squares regressions of each variable on swimming speed. To account for individual variation in motor patterns, the relationship of each variable with swimming speed was tested within individuals, using the sequential Bonferroni test (Sokal and Rohlf, 1994) to establish significance levels. All analyses were performed using JMP 3.1 (SAS Institute).

### Results

The basic pattern of muscle activity during pectoral locomotion in *Gomphosus varius* is that of alternating contractions of the abductor and adductor muscle groups at all

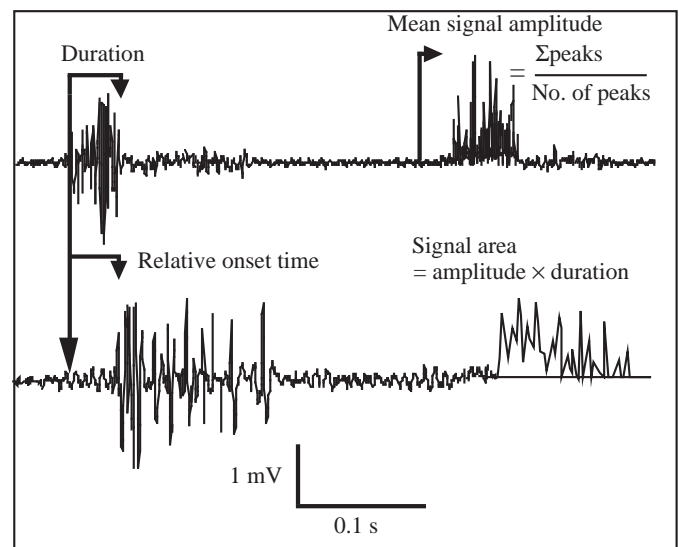


Fig. 3. Measurement of the EMG variables presented in this study, including duration, relative onset time, signal amplitude and signal area.

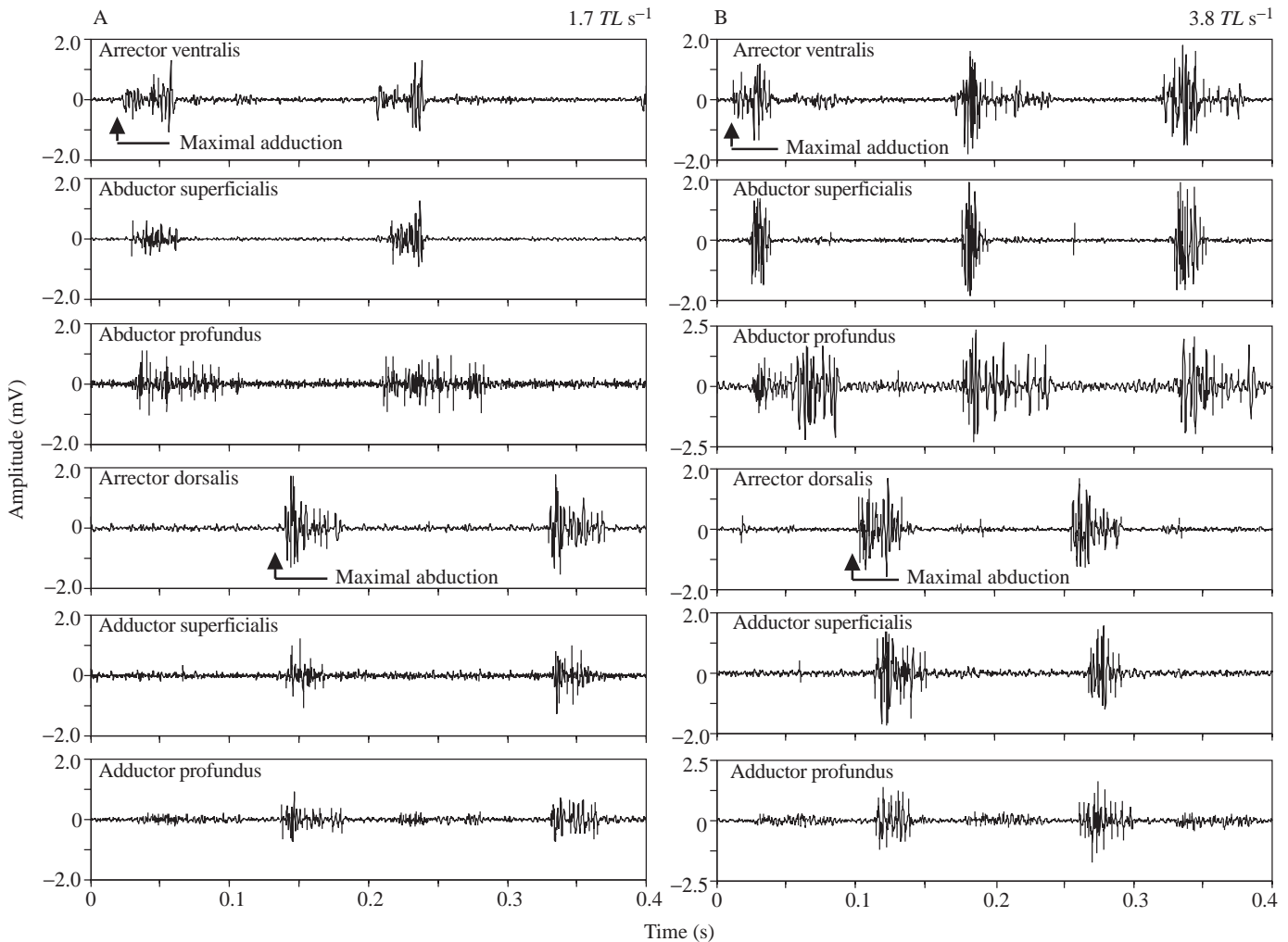


Fig. 4. Raw EMG data illustrating the profile of muscle activity for the pectoral fin stroke of *Gomphosus varius* at a relatively low speed (A) of  $1.7 \text{ TL s}^{-1}$  and at a higher speed of  $3.8 \text{ TL s}^{-1}$  (B). Noted on each profile are the times of maximal abduction (downstroke) and maximal adduction (upstroke).

swimming speeds. Most EMG variables showed significant trends with increasing swimming speed. The duration of activity and the relative onset times decreased as velocity increased, whereas the signal amplitude and the rectified EMG area of most muscles increased with swimming speed. Timing variables expressed as a fraction of stride period were less strongly correlated with velocity. Analysis of synchronized EMG and kinematic patterns reveals the timing of muscle activity relative to fin motion. The pectoral abductor and adductor muscles in *G. varius* are active in synchrony with the actions of fin abduction and adduction, respectively, allowing estimation of positive muscle work during swimming.

#### *Pectoral fin myology*

The descriptive anatomy of the pectoral girdle, pectoral musculature and fins in fishes has been founded on a strong comparative literature (Shann, 1920; Starks, 1930; Winterbottom, 1974; Geerlink, 1989). The morphology and mechanical design of the pectoral fin were described by

Westneat (1996), and the basic anatomy is presented here for *G. varius*. The pectoral girdle is the anchor upon which the pectoral muscles originate. The anteroventral surfaces of the cleithrum, both laterally and medially, as well as the scapula and coracoid, are the sites of attachment for the abductor and adductor musculature (Fig. 2). The first pectoral fin ray is a short, thick ray that articulates with the scapula in a synovial joint. The first and second pectoral rays are tightly connected by connective tissues to form a single rotational element that forms the leading edge of the pectoral fin (Fig. 2A). Pectoral rays 2–16 in *G. varius* have their bases embedded in a fibrous pad that separates them from the underlying radials. Pectoral fin shape is determined largely by relative fin ray length: the anterodorsal rays of *G. varius* are the longest, and the rays taper in length from dorsal to ventral, forming a wing-shaped fin.

Six major pectoral muscles actuate the fin during locomotion. Three muscles form the abductor complex that abducts the fin during the downstroke. The abductor superficialis and abductor profundus (Fig. 2A) are broad,

flattened muscles that originate on the anterolateral face of the cleithrum and insert *via* the abductor tendons onto pectoral rays 2–16. The arrector ventralis (Fig. 2B) also attaches along the anterolateral edge of the cleithrum, lying medial to the abductor superficialis. The arrector ventralis inserts onto the anterior base of the first pectoral ray by a stout tendon. The adductor complex (Fig. 2C,D) is composed of three major muscles and two smaller muscles. The adductors superficialis and profundus originate on the anteromedial surface of the cleithrum and insert *via* adductor tendons onto pectoral rays 2–16. These muscles are antagonists to the abductors superficialis and profundus. The adductor superficialis is folded upon itself in a complex manner, with a dorsal, medial portion that inserts onto fin rays 5–16 and a more ventral portion that inserts onto rays 2–4 in *G. varius* (Fig. 2D). The arrector dorsalis originates anteroventrally on the medial face of the cleithrum and inserts onto the anterior base of the first pectoral ray by a stout tendon, as an antagonist to the arrector ventralis. Other adductor muscles include the adductor radialis (Fig. 2C), originating on the caudal margins of the scapula and coracoid, inserting onto pectoral rays 14–16, and the coracobrachialis, attaching to the rear portion of the coracoid and ventral margin of the fourth radial.

*Synchronized EMG and kinematics: the motor pattern of labriform locomotion*

The overall pattern of pectoral muscle activity (Fig. 4) was that of activity in the three abductor muscles during the downstroke, followed by activity in the three adductors during the upstroke. Summary diagrams of EMG activity and the kinematic profile of the fin during slow swimming (Fig. 5A) and faster propulsion (Fig. 5B) illustrate the changes in timing and duration of muscle activity relative to fin motions. The arrector ventralis (AV) muscle began the fin-beat cycle, commencing activity between 3 and 55 ms after maximal adduction of the fin against the body (Table 1). The onset of AV activity occurred 3–18 ms (depending upon swimming speed) before the initiation of activity in the other abductors (Fig. 5; Table 2). The AV was active during the initial protraction of the fin forward along the body and then during the beginning of the downstroke, for a mean duration of 27 ms (Table 2). The abductor superficialis (AbS) and abductor profundus (AbP) began activity nearly synchronously with one another, between 3 and 18 ms after the onset of AV activity, and an average of 30 ms after maximal adduction of the fin (Table 1). These muscles were active during most of the downstroke of the pectoral fin (Fig. 5). The AbS muscle was active for an average of 28 ms and the AbP was usually active for longer, averaging 45 ms (Table 2). Electrical activity in all abductor muscles ended before maximal abduction of the pectoral fin (Fig. 5).

At or closely following the time of maximal pectoral fin abduction, the adductor muscles became active nearly simultaneously (Fig. 5). Activity in the arrector dorsalis often preceded activity in the other two adductors by several milliseconds, but the mean onset times were all approximately 128 ms after onset of activity in the AV (Table 2). The initial

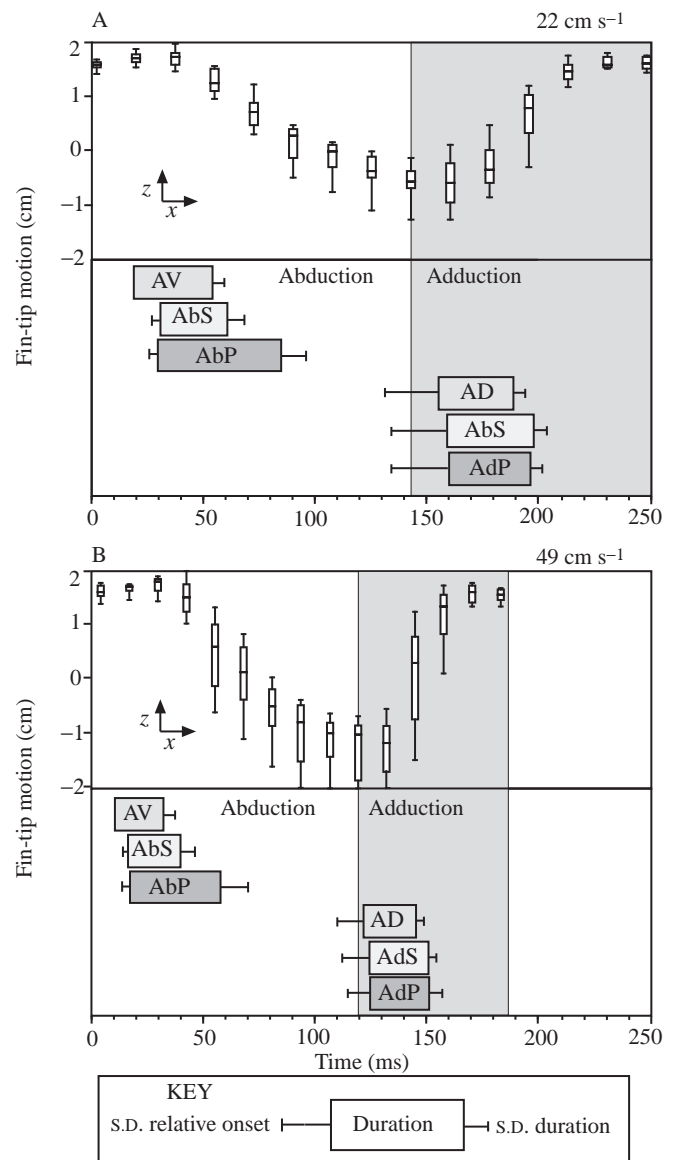


Fig. 5. Summary of *Gomphosus varius* synchronized kinematics and motor pattern at two swimming speeds. (A) 22 cm s<sup>-1</sup> (1.7 TL s<sup>-1</sup>); (B) 49 cm s<sup>-1</sup> (3.8 TL s<sup>-1</sup>). In the upper panel of each plot, fin-tip motion is shown in lateral view as the fish swims from left to right (see Walker and Westneat, 1997). Each plot represents the pooled distribution of all sequences and individuals. Error bars represent standard quartiles. In the lower panel are the summary motor patterns for all fish for all trials. Bar length indicates the mean duration of the EMG, the error bar to the left indicates the standard deviation of onset time, and the error bar to the right indicates the standard deviation of duration. AV, arrector ventralis; AbS, abductor superficialis; AbP, abductor profundus; AD, arrector dorsalis; AdS, adductor superficialis; AdP, abductor profundus.

activity of the adductors occurs during the 'fin flip' of the pectoral fin, in which the leading edge of the fin is rotated sharply dorsally and posteriorly. The adductors were active during most of the upstroke, their duration of activity lasting from 17 ms to 56 ms (Table 2). Adductor EMG activity ceased before maximal adduction (Fig. 5), although fin motion

continued smoothly until the fin was pressed against the body. No definite 'pause' phase was observed in *G. varius*, as has been documented in centrarchids (Gibb *et al.* 1994) and embiotocids (Drucker and Jensen, 1996; Webb, 1973), as the bird wrasse fin entered immediately into the next abduction phase at all steady swimming speeds.

*Trends in timing and duration with swimming speed*

Swimming velocity was a highly significant covariate with nearly all the measured EMG variables (Tables 1, 2). Of particular importance to an understanding of pectoral fin mechanics and muscle function is the timing of muscle activity relative to the times of reversal of fin motion during

Table 1. Mean, standard deviation and range of timing of muscle EMG onset relative to kinematic parameters for *Gomphosus varius*

Variable	Mean	S.D.	Range		Regression equation	$r^2$	P*
			Minimum	Maximum			
Adduction to onset AV (ms)	21.07	13.97	3.38	54.61	$y=-0.45x+38.3$	0.29	0.044 (2)
Adduction to onset AbS (ms)	29.91	16.28	9.18	69.05	$y=-0.66x+55.3$	0.47	0.007 (2)
Adduction to onset AbP (ms)	29.95	14.53	11.22	65.73	$y=-0.61x+53.1$	0.49	0.006 (2)
Adduction to onset AD (ms)	8.83	8.73	-1.07	31.78	$y=-0.37x+22.8$	0.32	0.005 (1)
Adduction to onset AdS (ms)	9.49	8.87	-0.67	28.42	$y=-0.30x+20.9$	0.32	0.034 (2)
Adduction to onset AdP (ms)	7.06	6.28	-2.05	17.01	$y=-0.32x+19.3$	0.73	<0.001 (2)

\*Number in parentheses is the number of individuals for which the relationship was significant; N=3 fish, 105 fin beats.

The onset of activity of the fin abductors was measured relative to maximal adduction.

The onset of activity of the fin adductors was measured relative to maximal abduction.

Regression equations,  $r^2$  values and significance levels are listed for the relationship between timing parameters and swimming velocity.

AV, arrector ventralis; AbS, abductor superficialis; AbP, abductor profundus; AD, arrector dorsalis; AdS, adductor superficialis; AdP, adductor profundus.

Table 2. Mean, standard deviation and range of electromyographic data for *Gomphosus varius*

Variable	Mean	S.D.	Range		Regression equation	$r^2$	P*
			Minimum	Maximum			
Duration AV (ms)	27.28	11.27	12.56	48.48	$y=-0.40x+41.92$	0.30	0.011 (3)
Duration AbS (ms)	27.89	6.52	19.04	43.28	$y=-0.25x+37.17$	0.36	0.005 (2)
Duration AbP (ms)	44.98	18.15	21.72	82.56	$y=-0.56x+65.35$	0.23	0.033 (0)
Duration AD (ms)	28.13	7.60	16.56	43.20	$y=-0.30x+39.28$	0.39	0.003 (2)
Duration AdS (ms)	32.70	10.74	19.64	55.72	$y=-0.32x+44.77$	0.24	0.029 (2)
Duration AdP (ms)	32.25	9.22	19.92	50.80	$y=-0.35x+45.22$	0.36	0.006 (2)
Onset of AbS to AV (ms)	8.80	3.71	3.28	15.40	$y=-0.21x+16.42$	0.76	<0.001 (3)
Onset of AbP to AV (ms)	8.41	3.28	3.84	17.88	$y=-0.14x+13.51$	0.43	0.002 (2)
Onset of AD to AV (ms)	127.52	21.48	95.20	167.44	$y=-0.84x+158.66$	0.38	0.004 (2)
Onset of AdS to AV (ms)	129.57	19.51	96.92	164.08	$y=-0.82x+158.41$	0.41	0.002 (2)
Onset of AdP to AV (ms)	128.24	20.97	96.84	172.60	$y=-0.93x+162.55$	0.48	<0.001 (3)
Amplitude AV (mV)	0.050	0.022	0.011	0.102	$y=-0.0008x+0.02$	0.32	0.009 (3)
Amplitude AbS (mV)	0.075	0.044	0.021	0.190	$y=-0.002x+0.012$	0.36	0.006 (3)
Amplitude AbP (mV)	0.079	0.037	0.029	0.169	$y=-0.002x+0.001$	0.78	<0.001 (3)
Amplitude AD (mV)	0.083	0.045	0.028	0.176	$y=-0.002x+0.006$	0.54	<0.001 (3)
Amplitude AdS (mV)	0.057	0.028	0.017	0.103	$y=-0.001x-0.002$	0.81	<0.001 (3)
Amplitude AdP (mV)	0.072	0.036	0.019	0.147	$y=-0.002x+0.008$	0.57	<0.001 (3)
Area AV (mV ms)	1.24	0.65	0.45	2.42	$y=-0.005x+1.08$	0.01	0.651 (1)
Area AbS (mV ms)	1.88	0.80	0.54	3.64	$y=-0.026x+0.92$	0.26	0.022 (2)
Area AbP (mV ms)	3.18	1.41	1.12	7.24	$y=-0.039x+1.74$	0.19	0.055 (2)
Area AD (mV ms)	2.14	1.06	0.70	4.90	$y=-0.030x+1.05$	0.19	0.050 (2)
Area AdS (mV ms)	1.66	0.65	0.81	3.16	$y=-0.031x+0.56$	0.54	<0.001 (2)
Area AdP (mV ms)	1.98	0.57	0.90	2.94	$y=-0.025x+1.05$	0.48	<0.001 (2)

\*Number in parentheses is the number of individuals for which the relationship was significant; N=3 fish, 105 fin beats.

Variables include muscle activity duration, onset time of five muscles relative to the arrector ventralis and two measures of EMG amplitude.

Regression equations,  $r^2$  values and significance levels are listed for the relationship between EMG parameters and swimming velocity.

See Table 1 for muscle abbreviations.

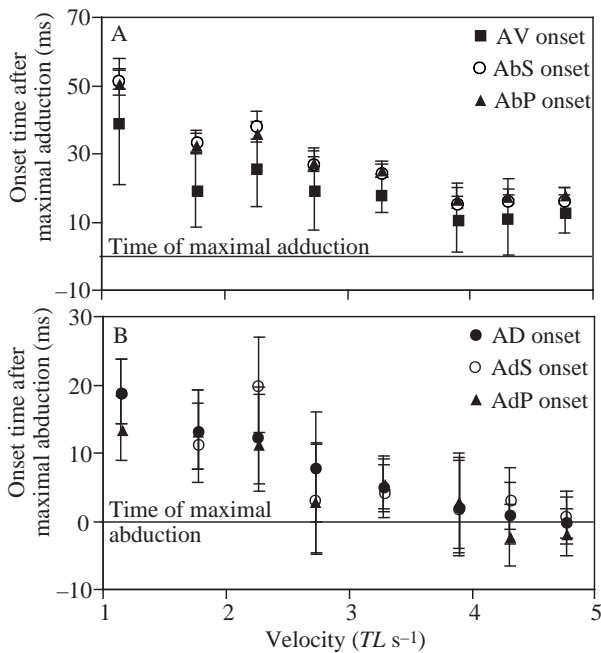


Fig. 6. Timing of EMG variables relative to maximal adduction and abduction plotted as a function of swimming velocity. The abductors (A) always begin their activity after maximal adduction, this delay decreasing with increasing swimming velocity. The adductors (B) also activate after maximal abduction, except at the highest speeds when peak downstroke and adductor initiation are nearly synchronous. Error bars signify standard deviation of the mean,  $N=3$  fish, 105 fin beats. See Fig. 5 for muscle abbreviations.

the flapping stroke. Fig. 6 illustrates these important timing events, showing that the abductors always began EMG activity after the moment of maximal adduction. This is true even of the arrector ventralis, in which the onset of activity occurs at least 3–5 ms after maximal adduction even at the

highest swimming speeds recorded. There was a significant negative slope to the relationship of these timing delays with swimming speed in all three abductors (Fig. 6; Table 1), indicating that the onset times occurred with less delay at higher speeds.

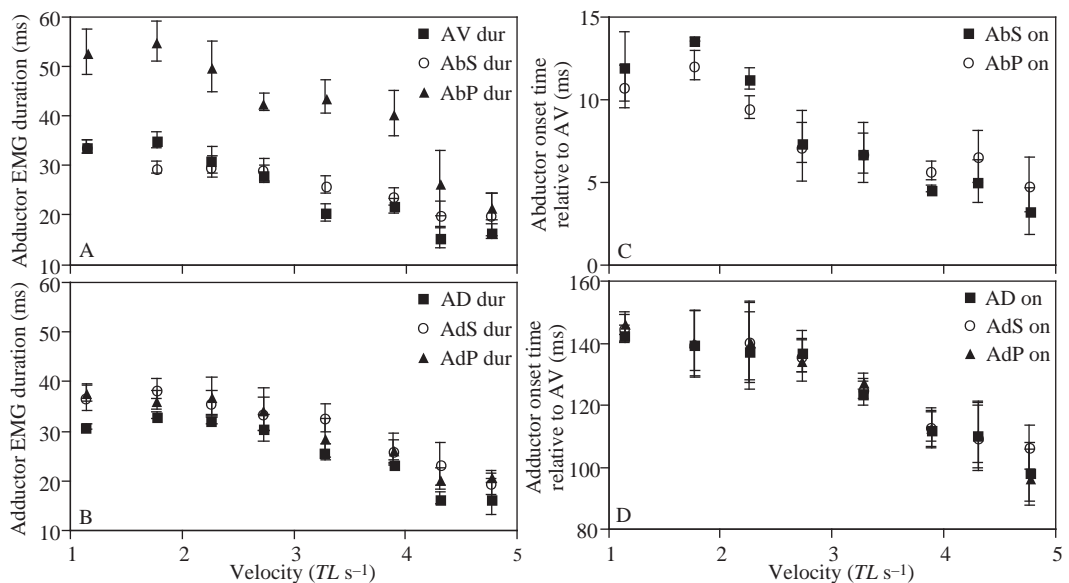
The adductor muscles also began activity after maximal abduction at most swimming speeds, but at the highest speeds the adductor muscles fired at or slightly before maximal fin abduction (Fig. 6). However, the adductors never began activity more than 2 ms before abduction (Table 1), and the major portion of their activity was during the upstroke at all swimming speeds (Figs 5, 6). The timing delay between maximal abduction and adductor activity also showed a significantly negative slope as swimming speed increased (Table 1).

The durations of muscle activity (in ms) decreased significantly in all muscles as swimming velocity increased (Fig. 7A,B; Table 2). Most of the pectoral fin muscles (except the abductor profundus) were active for a maximum of approximately 40 ms at slow speeds, with activity dropping to a minimum of 15–20 ms at high swimming speeds (Fig. 7). The duration of activity of the abductor profundus was greater than that of the other muscles (both abductors and adductors) at most swimming speeds (Fig. 7A).

The onset times (in ms) of muscles relative to the onset of activity in the arrector ventralis muscle (which starts the cycle) also showed strong negative correlations with swimming speed (Fig. 7B,C). The relative onset times of the two abductors decreased significantly with increasing velocity (Table 2), from a maximum of approximately 15 ms delay to a minimum of 3–5 ms delay after the onset of AV activity. Activity in the three adductor muscles showed decreasing time delays relative to AV onset, from approximately 150 ms to 100 ms (Fig. 7D).

An alternative way to examine muscle timing and duration is in relation to the stride period of the locomotor cycle. The stride duration, defined as the time between successive maximal

Fig. 7. (A,B) Trends in the duration (dur) of EMG activity in the pectoral muscles of *Gomphosus varius* as swimming velocity increases. The abductor profundus is active for longer than the other five muscles at all velocities. (C,D) Trends in the onset time (on) of EMG activity in the pectoral muscles relative to the onset of the arrector ventralis as swimming velocity increases. For both abductors and adductors, the delay relative to the AV muscle decreases with increasing speed. Error bars signify standard deviation of the mean,  $N=3$  fish, 105 fin beats. See Fig. 5 for muscle abbreviations.



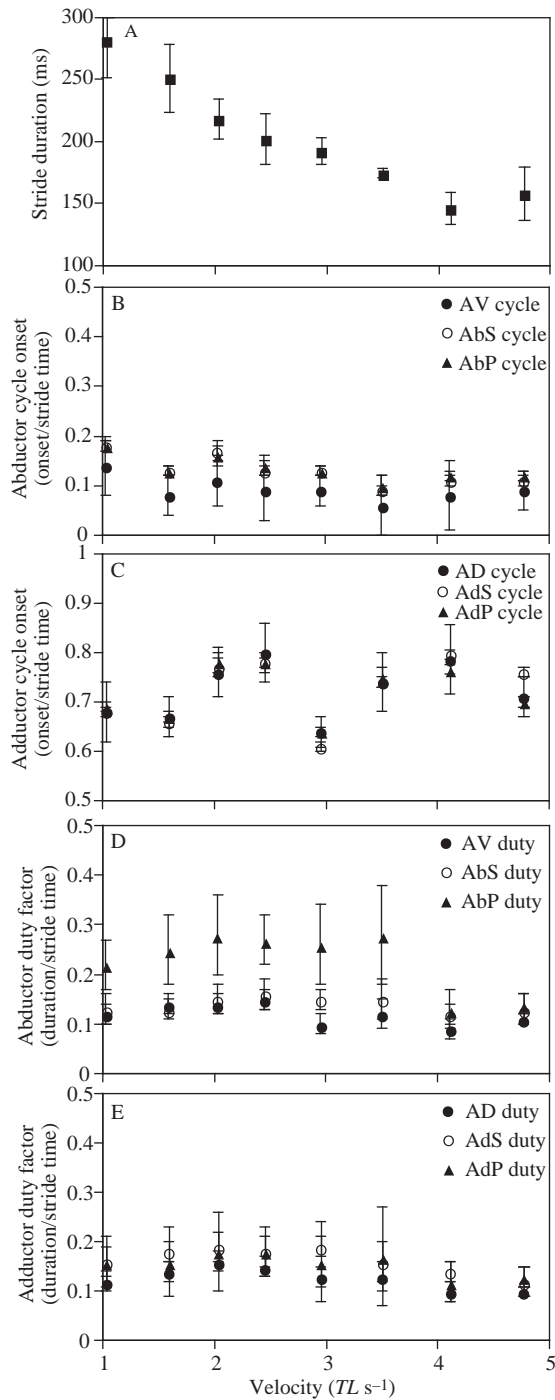


Fig. 8. Stride variables of the pectoral stroke of *Gomphosus varius* as swimming velocity increases. (A) Stride duration (in ms) at each swimming velocity. (B) The onset times of abductor muscles expressed as a fraction of the total stride duration at each velocity. (C) The onset times of adductor muscles expressed as a fraction of the total stride duration at each velocity. (D) The duty factors of abductor muscles, calculated as the muscle activity duration divided by total stride duration at each velocity. (E) The duty factors of adductor muscles, calculated as the muscle activity duration divided by total stride duration at each velocity. Error bars signify standard deviation of the mean,  $N=3$  fish, 105 fin beats. See Fig. 5 for muscle abbreviations.

adduction positions, decreases with increasing swimming speed (Fig. 8A). This variable, when expressed in seconds, is the inverse of fin-beat frequency. Despite the significant decrease in muscle onset times relative to kinematic reversal points (Fig. 6), the same onset data expressed as a fraction of the stride period show no significant slope (Fig. 8B,C). Thus, each muscle begins activity at the same relative point of the stride cycle regardless of swimming speed. The same is true for most of the duty factors of the pectoral muscles (Fig. 8D,E). Duty factors, expressed as the fraction of the stride period during which muscles were active, show no significant trend with swimming velocity, although the duty factor of the abductor profundus decreases at the two highest swimming speeds (Fig. 8D).

*Trends in contraction intensity with swimming speed*

The amplitudes of muscle activity (a measure of burst intensity) were measured as the mean signal height of each EMG trace (in mV) (Fig. 9A,B). Amplitude showed a significant, positive correlation with swimming velocity in all six muscles (Table 2). EMG amplitudes ranged in intensity from 0.02 mV at low speeds up to approximately 0.15 mV at high speeds. The abductor muscles, particularly the arrector ventralis (Fig. 9A), appeared to reach a maximal voltage beyond which no further increase occurred with increased speeds. The arrector ventralis voltage dropped slightly beyond a velocity of approximately  $4 TL s^{-1}$ . In contrast, the amplitudes of the adductor muscles showed a more linear increase with increasing velocity (Fig. 9B).

A second measure of the intensity of muscle activity is the rectified, integrated area of EMG signals, measured as the product of mean signal height and duration (mVms) (see Fig. 3). This parameter was less strongly associated with swimming velocity and showed higher variability among muscles (Fig. 9C,D). As swimming velocity increased, duration decreased and amplitude increased to yield a product that did not always correlate strongly with speed. Significant associations with speed were found for the abductor superficialis, adductor superficialis and adductor profundus (Table 2). Values for the other three muscles were not significantly correlated with speed below the 0.05 level, although values for the abductor profundus and arrector dorsalis were correlated at the 0.05 level. The abductor muscles again exhibited a maximal EMG area beyond which area leveled off or decreased as swimming velocity increased (Fig. 9C). The adductors showed a similar pattern, in which EMG area peaked at approximately 3 mVms at a speed of  $3.5 TL s^{-1}$ , beyond which no increase with speed was observed (Fig. 9D).

**Discussion**

The motor patterns of the six major muscles of the pectoral fin of the bird wrasse *Gomphosus varius* show strong correlations with swimming velocity and with fin kinematics. By interpreting the patterns of timing and intensity of the pectoral muscles in conjunction with the morphology and the kinematics of the pectoral fin, we are able to interpret the

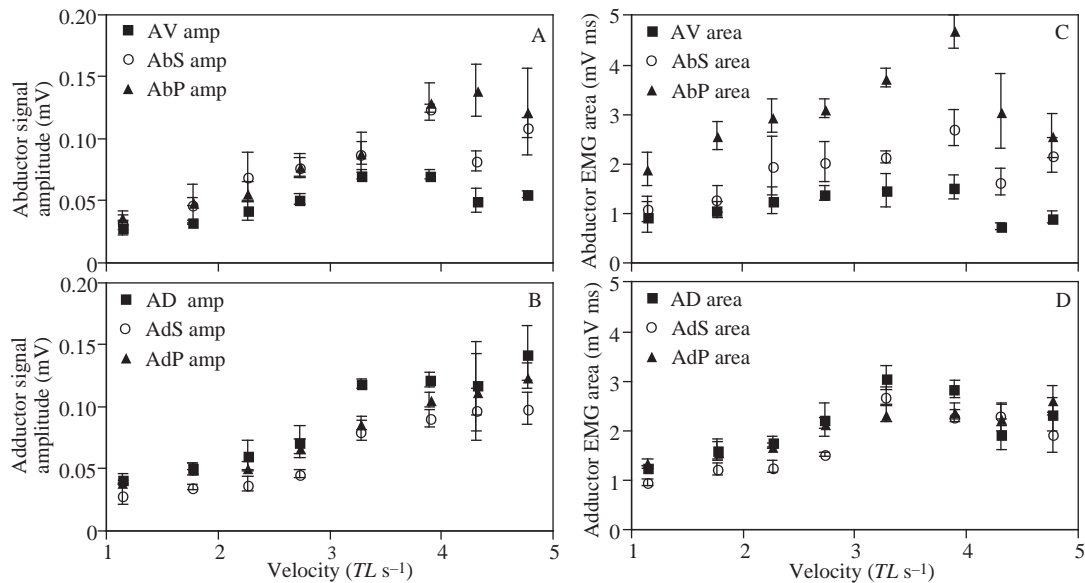


Fig. 9. (A,B) The amplitude (amp, mean voltage) of EMG signals increases with increasing swimming velocity. The abductors (A) appear to reach a maximal amplitude at approximately  $4.0 TL s^{-1}$ , whereas the amplitude of the adductors (B) increases linearly throughout the velocity range examined. (C,D) Trends in the rectified, integrated area of EMG activity in the pectoral muscles of *Gomphosus varius* as swimming velocity increases. In this estimate of muscle contraction intensity, both abductors (C) and adductors (D) reached a maximal EMG area at  $3-4 TL s^{-1}$ , beyond which no increase was observed. Error bars signify standard deviation of the mean,  $N=3$  fish, 105 fin beats. See Fig. 5 for muscle abbreviations.

biomechanics of pectoral musculoskeletal function. Of particular importance is the resolution of the timing of the onset of muscle activity relative to the initiation of the downstroke and upstroke of pectoral propulsion, as these data allow us to infer the role of muscles in generating the work and power required for propulsion. In addition, the correlation of EMG and kinematic patterns across velocities can identify the role of neuromuscular function in behavioral changes associated with the transition from low to high swimming velocity.

#### *How pectoral fins work: mechanical design, kinematics and motor patterns*

A full understanding of the functional morphology of a complex musculoskeletal system requires information regarding the anatomical design of the system, the motion of the system during the behavior of interest, physiological data on muscle contraction patterns and muscle contractile properties, and other data such as the mechanical properties of tissues. Several previous studies have focused on pectoral fin anatomy (Shann, 1920; Starks, 1930; Winterbottom, 1974; Geerlink, 1989) and kinematics (Webb, 1973; Gibb *et al.* 1994; Drucker and Jensen, 1996; Lauder and Jayne, 1996; Walker and Westneat, 1997), allowing correlation of some aspects of structure with fin function. Westneat (1996) further outlined the mechanism of pectoral motion by combining preliminary kinematic and EMG data for *G. varius* with a three-dimensional mechanical model of the pectoral fin. We use the present data on the patterns of onset and intensity of activity in the pectoral muscles, correlated with fin motion, to interpret

the role of neuromotor patterns in the mechanism of labriform locomotion.

The basic motor pattern of pectoral propulsion is that of alternating activity of the antagonistic abductor and adductor muscle groups (Figs 4–6). Starting at the point of maximal adduction with the fins against the body, EMG activity begins with the firing of the arrector ventralis muscle before the other abductors. The arrector ventralis functions to initiate the peel of the leading edge of the fin away from the body to begin the propulsive downstroke. The AV is active through the initial stages of abduction, with activity ending well before maximal abduction (Figs 5, 6). Before the downstroke begins, however, the fin is protracted without lateral motion (Walker and Westneat, 1997). The arrector ventralis may act as a fin protractor at higher speeds, pulling the fin forward while it is pressed against the body, but the AV muscle is not usually active during this behavior, and none of the other muscles recorded is active at this point. We suggest two hypotheses for the cause of fin protraction to begin the fin beat. The action could be the fin returning passively to its rest position, pulled forward by strains in the heavy tendons of the abductor muscles that attach to its leading edge. Another possibility is that the dorsal portion of the adductor superficialis, oriented at right angles to the ventral portion of the AdS and inserting on the posterior fin rays, functions as a fin protractor rather than a fin adductor. Testing this hypothesis would require an EMG recording from this portion of the muscle.

The abductor superficialis and abductor profundus act in concert with the arrector ventralis to produce the downstroke of the fin. These large bands of muscle always initiate activity

after the arrector ventralis has pulled the leading edge of the fin away from the body and started the downstroke (Fig. 5). This pattern of early AV activity and delay in contraction of the other abductors may correlate with the anatomy of the tendinous attachments of the three muscles to the bases of the fin rays. The AV attaches only to an anterolaterally directed process on the first pectoral ray (Geerlink, 1989; Westneat, 1996). This large process represents an effective lever arm for the AV muscle to gain the appropriate mechanical advantage for the initiation of the downstroke. The tendons of AbS and AbP attach to the bases of pectoral rays 2–16. These fin rays have short, ventrolaterally directed processes to accept the tendons of the abductors as they course over the thick fibrous pad upon which the fin rays rotate (Fig. 2B). It is likely that the mechanical advantage of the major abductors at full fin adduction is poor because of the relatively shorter lengths of the processes on the fin ray bases. However, once the downstroke has begun, any loss of mechanical advantage is traded for a relatively higher displacement advantage that enables these muscles to abduct the fin with greater speed.

As the downstroke ends and the fin approaches maximum abduction, none of the muscles we recorded was active except at the highest speeds measured, when the adductors fired 1–2 ms before maximal abduction (Fig. 6). The mechanism of fin deceleration thus remains unknown: possible explanations include stretching of the ligaments that bind the anterior fin rays to the pectoral girdle (Geerlink, 1989), passive deceleration due to drag, or contraction of the two smaller pectoral adductor muscles not measured here.

Immediately following maximum abduction, the upstroke begins with the ‘fin flip’, in which the leading edge is rotated sharply dorsally and posteriorly and the trailing edge continues forwards and downwards to change the angle of attack of the fin rapidly (Walker and Westneat, 1997). This action is initiated by activity of the arrector dorsalis muscle (AD), which usually begins activity slightly before the other adductors. The AD, like the AV, attaches only to a process on the base of the first pectoral ray. At full abduction, the action of the AD produces a force on the leading edge of the fin through the moment arm of the process on the ray base. The adductors superficialis and profundus are active in synchrony with fin adduction. The bony processes to which the AdS attaches are fairly distal to the base of the fin rays, giving the muscle a long moment arm and a high mechanical advantage. In contrast, the processes to which the AdP attaches are short, close to the base of the ray and ventrolaterally directed (Westneat, 1996). The AdP thus has a relatively poorer force transmission capability but an enhanced ability to transmit motion to fin rotation.

During steady forward swimming, neuromuscular activity controls the six major muscles of the fin to produce a repetitive flapping motion in which forward thrust is generated during both downstroke and upstroke (Walker and Westneat, 1997). The bird wrasse has fine motor control over the leading edge owing to the independent AV and AD muscle antagonists. Additionally, the muscles that drive the other fin rays are individually specialized for transmission of force or

displacement at particular times of the stroke cycle. This flexibility of motor control and the biomechanics of muscle transmission are certain to be critical to turning and complex maneuvers.

#### *Kinematics, swimming velocity and motor control of the pectoral fin*

The frequency and amplitude of EMG activity in *Gomphosus varius* pectoral muscles increased with increasing swimming speeds. This trend is clearly associated with the requirement for the faster, more forceful, muscle contractions necessary to drive the fin through its propulsive stroke at the increasing frequencies observed in the kinematic profiles of this species. Despite the significant trends in onset times and durations of muscle activity with increased velocity of swimming (Figs 6, 7), a remarkably consistent pattern emerges when these factors are calculated as onset points and activity ranges within the stride cycle (Fig. 8). Across a broad range of swimming speeds, the stride cycle onset and the duty factors of the pectoral muscles remain fairly constant, raising questions regarding the interaction between neural control and the detailed kinematics of the pectoral stroke at different speeds. Walker and Westneat (1997) demonstrated that several important kinematic features of the fin beat are dependent upon the velocity of propulsion. The underlying morphological, mechanical or neuromotor causes of these trends in kinematics of the stroke in *G. varius* require explanation.

The stroke plane angle ( $\beta$ ) of the bird wrasse represents the oscillatory motion of the leading edge of the fin relative to the longitudinal body axis and the flow of water (Fig. 3 in Walker and Westneat, 1997). This parameter shows no significant change with forward speed, remaining at approximately  $20^\circ$  from the vertical across individuals and speeds. The stroke plane of a fin beat is determined by several morphological factors, including the orientation of the fin base and the shape of the saddle joint between the base of the leading-edge ray and the scapula (Geerlink, 1989). In addition,  $\beta$  depends on the actions of the arrector ventralis and dorsalis muscles on the base of the first pectoral ray. Presumably, altering the relative timing and duty cycle of the arrector muscles could change the stroke plane angle by pulling the fin further forward or adducting it further posteriorly. The constant onset cycles and duty factors of these muscles across speed-dependent stride periods maintain a relatively constant stroke plane, a result consistent with our conclusion that *G. varius* generates lift during both upstroke and downstroke at all forward speeds.

In contrast to stroke plane angle, the angular amplitude of the stroke ( $\Phi$ ) increases with swimming velocity across most of the range of speeds examined (Fig. 4 in Walker and Westneat, 1997). Stroke amplitude might be modified by changes in relative timing of muscles (longer abductor duration or later adductor onset) or by increasing muscle force for abduction. We conclude that stroke amplitude is proportional to the total muscle force exerted on the fin. Our results show increases in EMG amplitudes and in some integrated areas, suggesting that more muscle fibers are recruited at higher

speeds (Fig. 9). This results in greater total force exerted on the fin ray bases. This force is exerted in a relatively constant duty cycle for each muscle across swimming speeds (Fig. 8). Owing to the range of insertion points of various muscles, increased muscle tension will be transmitted as both higher force transmission and higher velocity of fin translation through the water.

The pectoral fin of *G. varius* heaves and pitches as it oscillates through the downstroke and upstroke, exhibiting a complex pattern of phase lag between the leading and trailing edges of the fin (Fig. 8 in Walker and Westneat, 1997). The relative motions of the leading and trailing edges are indicative of the hydrodynamic chords of the fin and reflect the three-dimensional angle of attack of the fin surface with respect to the fish's body and the direction of water flow (Fig. 13 in Walker and Westneat, 1997). Our EMG data cannot be used to associate neuromotor patterns with these finer details of fin motion because we recorded muscle activity from a single, central location in each of the pectoral muscles. The complex twisting of the fin, the phase lag between the leading and trailing edges and the important hydrodynamic angles of attack are probably a product of the mechanical properties (flexural stiffness, elasticity) of the fin rays and the fin membrane as well as differential patterns of contraction of muscle fiber bundles within each muscle. Future work is needed in which multiple electrodes are implanted in different locations within major muscles to search for motor patterns that correlate with fin shape at different times of the stride period.

#### *Muscle work and the energetics of labrid pectoral fins*

The work performed and the power of muscle in an oscillatory locomotor system are dependent upon the cycle frequency, the timing of activation, the duty factors and contraction kinetics such as the force/velocity curve and the relaxation time of muscle (Josephson, 1985). These factors determine the association between the active period of a muscle and the speed and distance that the muscle can contract (for positive work) or be stretched (for negative work). Many of these factors have been measured during previous work on bird flight (Dial *et al.* 1991; Tobalske, 1995), insect flight (Mizisin and Josephson, 1987; Tu and Dickinson, 1994) and undulatory axial locomotion in fishes (Altringham *et al.* 1993; Rome *et al.* 1993; Jayne and Lauder, 1995; Wardle *et al.* 1995). In particular, EMG patterns and *in vitro* physiological studies of muscle fibers (work-loop studies) have clarified the role of muscles in oscillatory musculoskeletal function. Our results on the motor patterns of pectoral swimming allow us to begin to consider muscle function in labriform locomotion.

The motor activity of the abductor muscles is synchronous with the onset and action of abduction, and adductor EMG activity is synchronous with adduction (Fig. 5). If force generation in the muscle occurs synchronously with EMG activity, then the pectoral muscles of *G. varius* perform positive work at all swimming speeds measured. Thus, the mechanism of pectoral propulsion in *G. varius* appears to involve no active deceleration of the fin by muscle at either

maximal downstroke or maximal upstroke and no preloading of muscles or tendons for increased stroke force.

A work-loop study of pectoral muscle in the sunfish *Lepomis gibbosus* supports this result (Luiker and Stevens, 1993). Sunfish pectoral muscle was oscillated at frequencies of 1–8 Hz, at duty factors of 8–32% of the stride period. These frequencies and duty factors are similar to those measured for *G. varius* EMGs (Fig. 8). At 1 Hz, the sunfish muscle did positive work at all duty factors and the net work was positive at all cycle frequencies examined. Some negative work was done at cycle frequencies above 1 Hz, but the maximal naturally occurring stride frequency for steady pectoral swimming in centrarchid fishes (basses and sunfishes) is approximately 1 Hz (Gibb *et al.* 1994; Lauder and Jayne, 1996). The highest frequency at which our EMG data were recorded was approximately 6 Hz, at which the adductor muscles began to fire a few milliseconds before adduction had begun, possibly producing a small amount of negative work. We have seen small *G. varius* beat their wings at 8 or even 10 Hz, possibly involving more negative work than at lower speeds. *G. varius* pectoral muscle is deep red in color and is probably largely composed of aerobic fibers. Fiber typing and work-loop studies of this muscle would allow accurate calculation of the work, power and swimming efficiency in this high-performance labriform swimmer.

In summary, our results on the patterns of EMG activity of the pectoral muscles supply an important component in our understanding of locomotor function. Using these data in conjunction with the morphology and the kinematics of the pectoral fin, we are able to interpret the biomechanics of pectoral musculoskeletal function. In addition, these data allow us to infer the role of muscles in generating the work and power required for propulsion by the pectoral fins over a wide range of speeds. We hope that these data lay a foundation for comparative work on the neuromotor basis of large-scale differences in labriform locomotion, such as rowing and flapping mechanisms, across diverse groups of fishes.

Special thanks to the Field Museum Biomechanics Group (M. Alfaro, S. Geick, M. Hale, J. Janovetz, L. Rosenberger, M. Pizer and B. Wright) for their help with this project. Thanks to M. Hale, E. Drucker and the anonymous reviewers for comments on the manuscript. This research was funded by National Science Foundation grant IBN-9407253 to M.W.

#### References

- ALTRINGHAM, J. D., WARDLE, C. S. AND SMITH, C. I. (1993). Myotomal muscle function at different locations in the body of a swimming fish. *J. exp. Biol.* **182**, 191–206.
- BLAKE, R. W. (1983). *Fish Locomotion*. Cambridge: Cambridge University Press.
- DANIEL, T. L. (1984). Unsteady aspects of aquatic locomotion. *Am. Zool.* **24**, 121–134.
- DANIEL, T. L. AND MEYHOFER, E. (1989). Size limits to escape locomotion of caridean shrimp. *J. exp. Biol.* **143**, 245–266.

- DIAL, K. P., GOSLOW, G. E. AND JENKINS, F. A., JR (1991). The functional anatomy of the shoulder of the European starling (*Sturnus vulgaris*). *J. Morph.* **207**, 327–344.
- DRUCKER, E. G. AND JENSEN, J. S. (1996). Pectoral fin locomotion in the striped surfperch. I. Kinematic effects of swimming speed and body size. *J. exp. Biol.* **199**, 2235–2242.
- DRUCKER, E. G. AND JENSEN, J. S. (1997). Kinematic and electromyographic analysis of steady pectoral fin swimming in the surfperches. *J. exp. Biol.* **200**, 1709–1723.
- GEERLINK, P. J. (1983). Pectoral fin kinematics of *Coris formosa* (Teleostei, Labridae). *Neth. J. Zool.* **33**, 515–531.
- GEERLINK, P. J. (1989). Pectoral fin morphology: a simple relation with movement pattern? *Neth. J. Zool.* **39**, 166–193.
- GIBB, A. C., JAYNE, B. C. AND LAUDER, G. V. (1994). Kinematics of pectoral fin locomotion in the bluegill sunfish *Lepomis macrochirus*. *J. exp. Biol.* **189**, 133–161.
- JAYNE, B. C. AND LAUDER, G. V. (1995). Are muscle fibers within fish myotomes activated synchronously? Patterns of recruitment within deep myomeric musculature during swimming in largemouth bass. *J. exp. Biol.* **198**, 805–815.
- JOSEPHSON, R. K. (1985). Mechanical power output from striated muscle during cyclic contraction. *J. exp. Biol.* **114**, 493–512.
- LAUDER, G. V. AND JAYNE, B. C. (1996). Pectoral fin locomotion in fishes: testing drag-based models using three-dimensional kinematics. *Am. Zool.* **36**, 567–581.
- LUIKER, E. A. AND STEVENS, D. (1993). Effect of stimulus train duration and cycle frequency on the capacity to do work in the pectoral fin muscle of the pumpkinseed sunfish, *Lepomis gibbosus*. *Can. J. Zool.* **71**, 2185–2189.
- MIZISIN, A. P. AND JOSEPHSON, R. K. (1987). Mechanical power output of locust flight muscle. *J. comp. Physiol. A* **160**, 413–419.
- ROME, L. C. AND SWANK, D. (1992). The influence of temperature on power output of scup red muscle during cyclical red muscle. *J. exp. Biol.* **171**, 261–281.
- ROME, L. C., SWANK, D. AND CORDA, D. (1993). How fish power swimming. *Science* **261**, 340–343.
- SHANN, E. W. (1920). The comparative myology of the shoulder girdle and pectoral fin of fishes. *Trans. R. Soc. Edinb.* **52**, 531–570.
- SOKAL, R. R. AND ROHL, F. J. (1994). *Biometry*. New York: W. H. Freeman and Co.
- STARKS, E. C. (1930). The primary shoulder girdle of the bony fishes. *Stanf. Univ. Pub. Biol. Sci.* **6**, 147–239.
- TOBALSKE, B. W. (1995). Neuromuscular control and kinematics of intermittent flight in the European starling (*Sturnus vulgaris*). *J. exp. Biol.* **198**, 1259–1273.
- TU, M. S. AND DICKINSON, M. H. (1994). Modulation of negative work output from a steering muscle of the blowfly *Calliphora vicina*. *J. exp. Biol.* **192**, 207–224.
- VOGEL, S. AND LABARBERA, M. (1978). Simple flow tanks for research and teaching. *Bioscience* **28**, 638–643.
- WALKER, J. A. AND WESTNEAT, M. W. (1997). Labriform propulsion in fishes: kinematics of flapping aquatic flight in the bird wrasse *Gomphosus varius* (Labridae). *J. exp. Biol.* **200**, 1549–1569.
- WARDLE, C. S., VIDELER, J. J. AND ALTRINGHAM, J. D. (1995). Tuning in to fish swimming: body form, swimming mode and muscle function. *J. exp. Biol.* **198**, 1629–1636.
- WEBB, P. W. (1973). Kinematics of pectoral fin propulsion in *Cymatogaster aggregata*. *J. exp. Biol.* **59**, 697–710.
- WESTNEAT, M. W. (1996). Functional morphology of aquatic flight in fishes: Mechanical modeling, kinematics and electromyography of labriform locomotion. *Am. Zool.* **36**, 582–598.
- WINTERBOTTOM, R. (1974). A descriptive synonymy of the striated muscles of the Teleostei. *Proc. Acad. nat. Sci. Philadelphia* **125**, 225–317.